IEEE Access
Multidisciplinary | Rapid Review | Open Access Journal

Received 1 December 2023, accepted 13 January 2024, date of publication 22 January 2024, date of current version 30 January 2024.

Digital Object Identifier 10.1109/ACCESS.2024.3357239

RESEARCH ARTICLE

GaN Transistors' Radiated Switching Noise Source Evidenced by Hall Sensor Experiments Toward Integration

VLAD MARSIC, SOROUSH FARAMEHR, JOE FLEMING, ROHIT BHAGAT, AND PETAR IGIC
Centre for Advanced Low Carbon Propulsion Systems, Institute for Clean Growth and Future Mobility, Coventry University, CV1 5FB Coventry, U.K.

Corresponding author: Vlad Marsic (vlad.marsic@coventry.ac.uk)

This work was supported by the Engineering and Physical Sciences Research Council (EPSRC) U.K. under Grant EP/V026577/1.

ABSTRACT Wide bandgap Gallium Nitride (GaN) technology promises to deliver the next generation of power transistors capable of high energy density and compact design integration however, without active monitoring high failing rates are recorded due to its instability to design parameter variations. Moreover, the electromagnetic (EM) radiofrequency (RF) emissions due to GaN power switching require extra design resources. Considering the extensive research area dedicated to galvanic isolated magnetic sensors for GaN wafer monolithic integration with usage in power monitoring, this study investigates the conditions that a Hall sensor is required to meet when operating in close proximity of a GaN transistor. Through considerable experimental testing, it was determined that the sensor requires a magnetic field starting from ± 1 mT when interfaced with a microcontroller. Additionally, since the GaN transistor's EM RF switching noise was one of the most monitored parameters during the experiments, it was discovered that it is proportional to the transistor's current transfer area whereas its magnitude is due to electrical current required by the load. As a result of these findings, the EM radiated switching noise may apply to all electrical switches and provide a significant advantage when designing for EM compatibility (EMC).

INDEX TERMS EMC/EMI, GaN transistor, hall sensor, magnetic field, RF emissions.

I. INTRODUCTION

Sensor embedding is the next evolution leap for previous technology, enabling real time monitoring and control. Integrating sensors in smart city's infrastructure [1], [2] and transportation routes for health monitoring [3], harvesting the environmental energy [4], [5] or equipped with powerful batteries for reliability such as for road traffic monitoring [6] or parking occupancy [7] upgrade previous technology and connects it to the new wave of internet of things (IoT) [8]. In the energy system, embedding sensors inside the rechargeable batteries used for e-mobility, to increase battery's life [9] decrease charging time [10] and reduce thermal runaway through in-situ monitoring [11] proved to be an efficient progressive measure. In addition, embedded communications on power lines like for electric cars [12] with a minimum of interfacing for wireless [13] or wired [14] transceivers since the DC power line shows no impact on its overall impedance [15], [16] constitutes another level of fusion and integration.

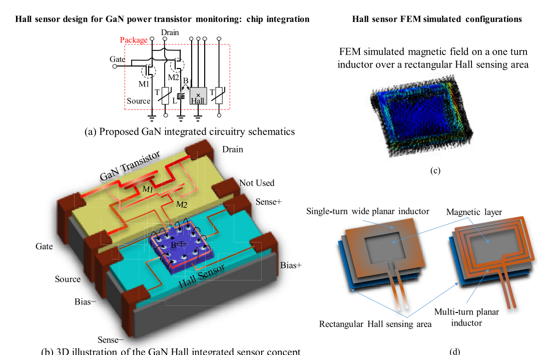

FIGURE 1. On-chip low power monitoring system designed for integration with GaN transistor: electrical schematics (a), general concept (b), magnetic field simulation for a rectangular inductor (c) and equivalent inductor configurations with magnetic layer (d).

The associate editor coordinating the review of this manuscript and approving it for publication was Ali Raza.

© 2024 The Authors. This work is licensed under a Creative Commons Attribution 4.0 License.
For more information, see https://creativecommons.org/licenses/by/4.0/

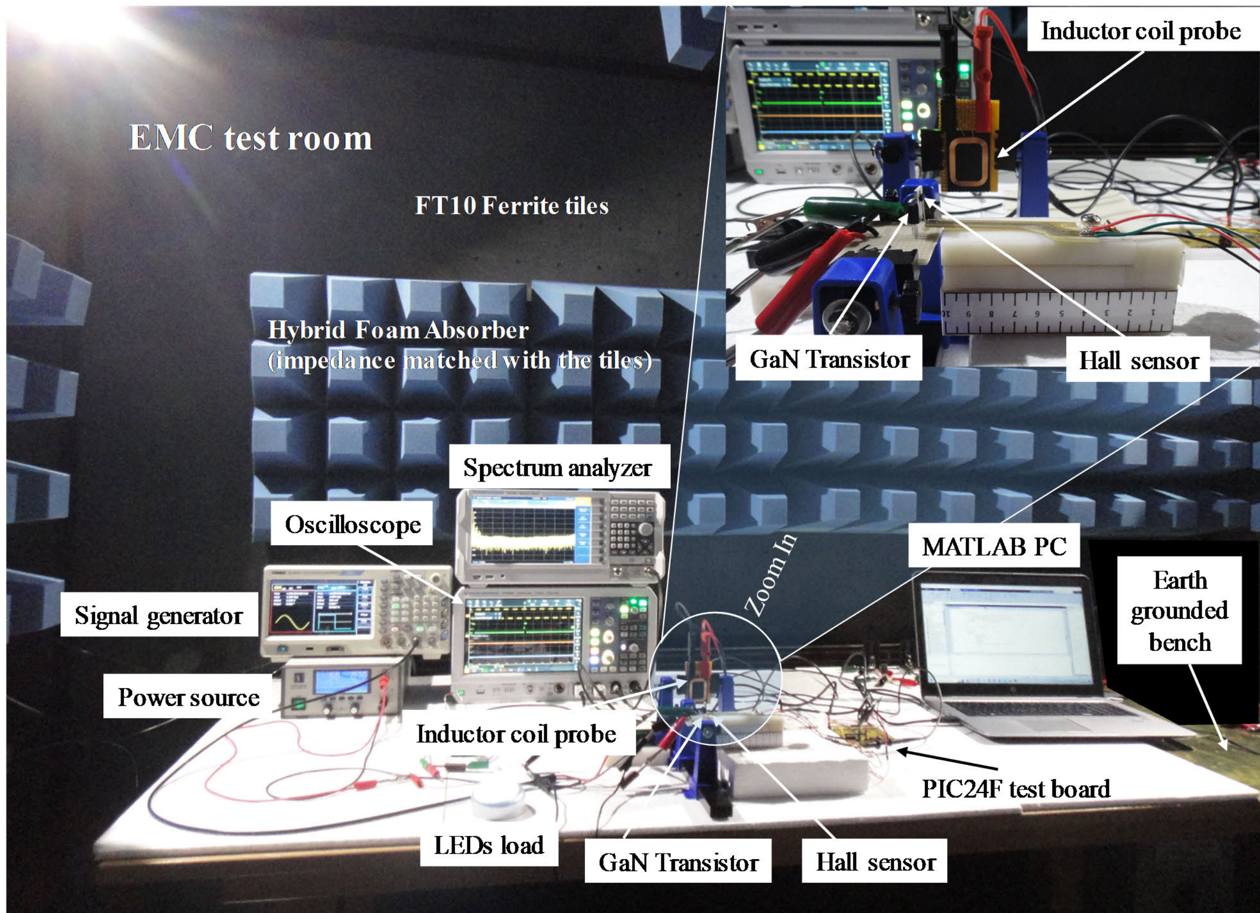

FIGURE 2. The GaN power transistor – Hall sensor experimental setup inside the EMC test room.

As miniaturisation and increased power density are acknowledged evolutionary paths in the world of power electronics, gallium nitride (GaN) transistor technologies emerge as a leading contender [17], [18], [19]. However, GaN transistors' functioning is susceptible to various unwanted effects resulted from their intricate structure [20].

Among these effects are signal reflections, which can trigger false ON/OFF regimes and cause the gate to unbalance [21] whereas radiating a large amount of radio frequency (RF) electromagnetic (EM) interferences (EMI) [22], [23].

This is why, current extensive research focuses on studying active monitoring and control methods for the GaN transistors [24], [25], via simulation [26], [27] and equivalent circuit experiments since integrated circuits (ICs) based on GaN technology involves a more difficult process [28], [29] as compared with its predecessor Silicon chips [30] or to the more exotic technology like diamond based semiconductors [31], [32]. Additionally, since the power designs based on GaN transistor technologies are very sensitive to external monitoring circuits that may limit the design performance [33], galvanically isolated sensors [34], [35] with magnetic coupling [36], [37], [38] are the next promising solution.

As the primary application of GaN transistor's technology is power switching, radiated EMI during switching is a major concern for low power chip-integrated sensors and their neighbor circuits located in close proximity to the transistor. Furthermore, despite the fact that radiated EMI is a feature of all power switches, the underlying mechanism and origin are still not well understood, with most EMC designs employing EMI filters, decoupling capacitors, electric shielding, RC snubbers, heatsink isolation, PCB ground rerouting and ferrite beads solely to mitigate the effects of produced RF noise but not the cause.

Through experimental testing, this study extends the simulation work described in [39], Fig. 1, to determine the minimum magnetic field density (B) value required by a generic Hall sensor for current monitoring in the noisy EM RF presence of a GaN transistor. As part of this analysis, seven test frequencies starting from 1, 5, 10, 50, 100, 500 up to 1000 kHz were used on three different loads, semiconductive, inductive and resistive whereas the Hall sensor have been interfaced with a microcontroller and an oscilloscope respectively. Since the GaN transistor's EM RF emissions have been carefully monitored inside an EM compatibility (EMC) room during the experiments, a legitimate observation

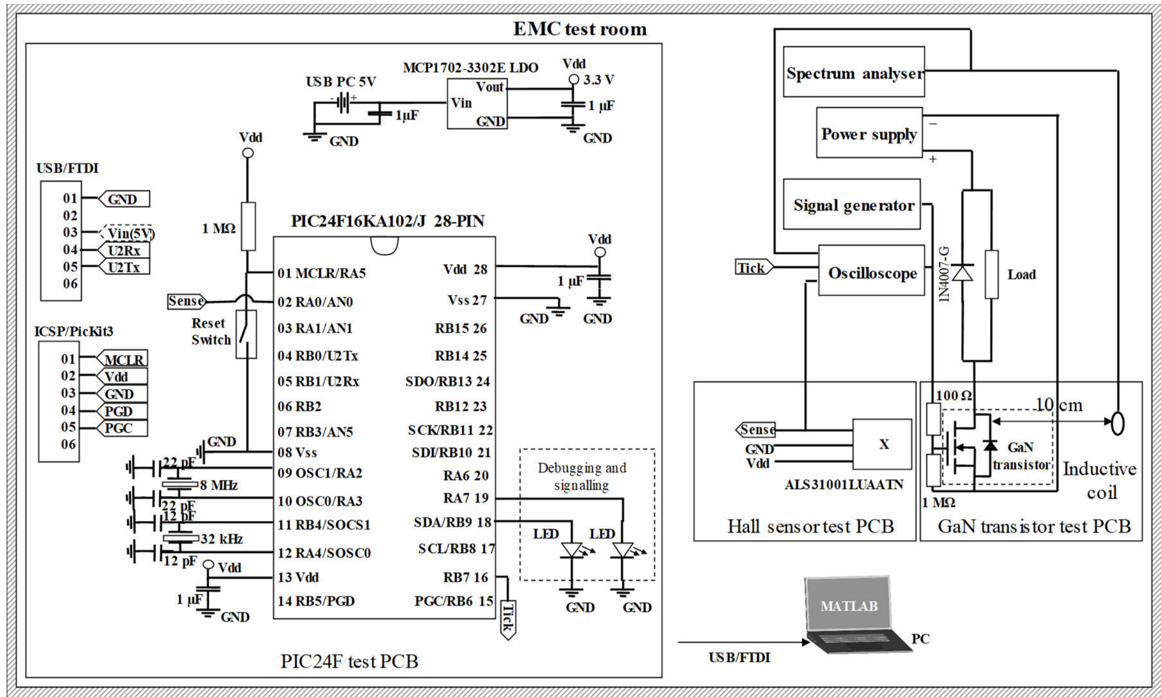

FIGURE 3. The GaN power transistor – Hall sensor experimental setup schematics inside the EMC test room.

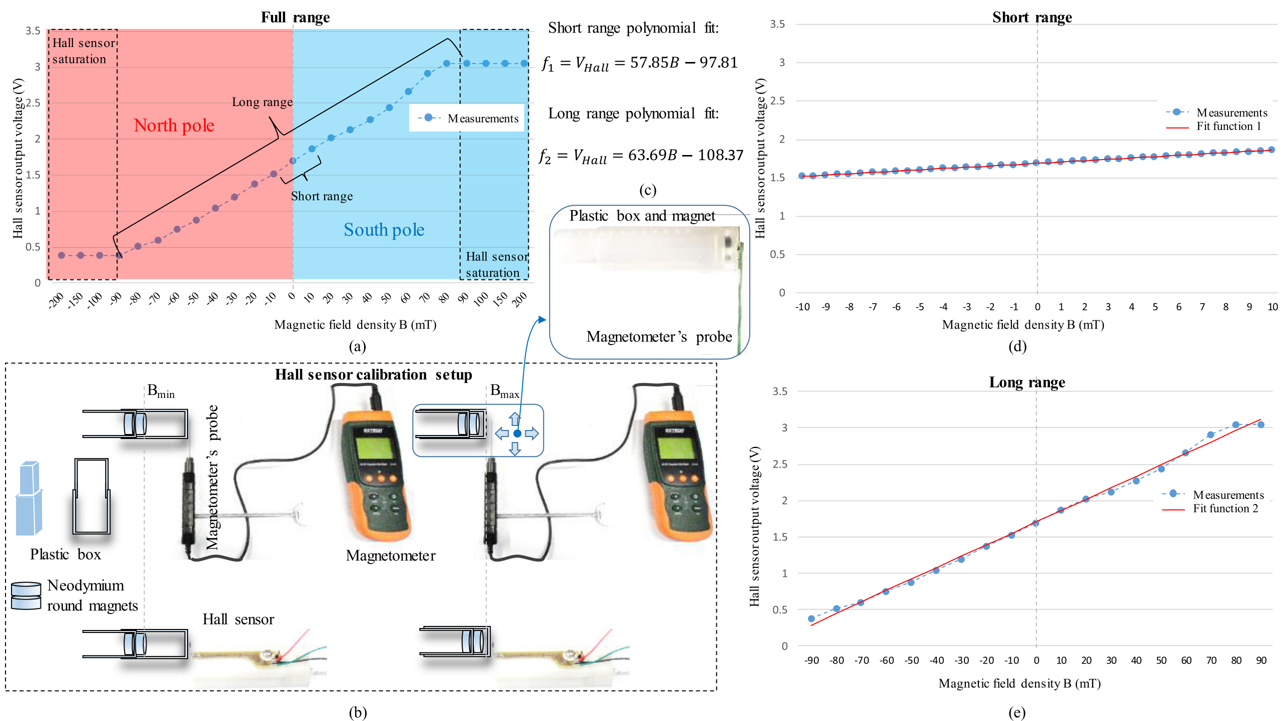

FIGURE 4. Hall sensor voltage vs magnetic field density overall results obtained during calibration (a), the calibration setup involving the magnetometer and microcontroller interfaced Hall sensor (b), the fitting functions developed for short and long range measurements (c), short range results (d) and long range calibration results (e).

related to the cause for radiated switching emissions triggered a comparative set of tests between two similar GaN transistors. The new tests have provided empirical evidence suggesting that power transistors and by extension all electrical switches radiate EM RF switching noise proportional with their conduction current contact area at room temperature

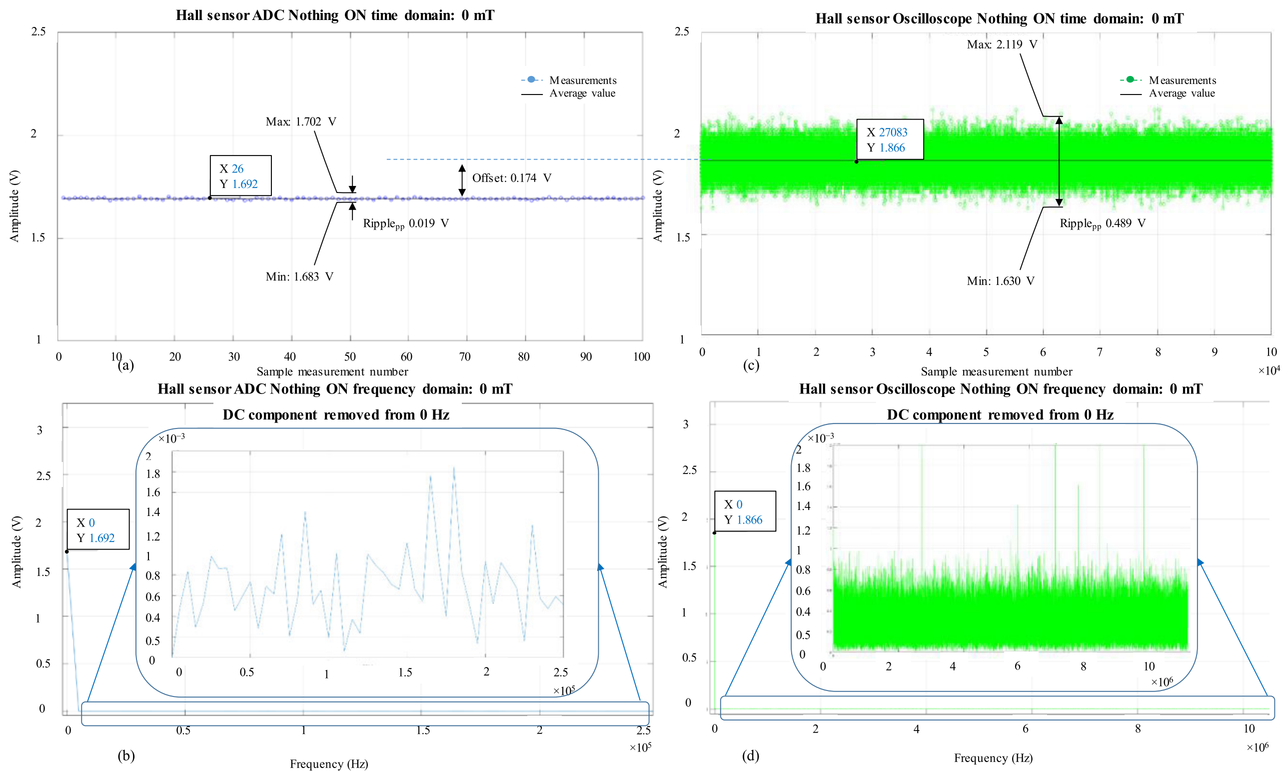

FIGURE 5. Measuring magnetic field with the Hall sensor interfaced by microcontroller in time domain (TD) (a) and frequency domain (FD) (b). Same tests interfacing the sensor with an oscilloscope in TD (c) and FD (d). It is showed that the average sensed field from TD is equal in amplitude at 0 Hz (DC) in FD.

without any special functioning conditions. Additionally, it was verified experimentally that up to 500 MHz spectrum is sufficient for monitoring of radiated EMI resulted from up to 1 MHz switching, supporting EMC/EMI investigations for this domain without requiring costly and labor-intensive setups for the GHz range.

Apart from establishing the detection limits for possible embeddable GaN Hall sensors for power monitoring, this study's results offer a valid explanation for the EM RF switching noise created by the electric switches. Due to the various models, materials, and geometries used in electrical switches, obtaining a valid generalized model relating to their spatial characteristics and RF emissions is an intricate task. Based on the findings of this work, a rule of thumb can be extrapolated to be used in EMC-sensitive designs in the future. Furthermore, by providing a path to the core cause and indicating that investigations in this field are not limited to expensive EMC equipment and facilities, these key findings may catalyst the development of novel solutions in power switching EMI reduction.

II. METHODOLOGY

All GaN transistor – Hall sensor experiments were conducted inside the Centre for Advanced Low Carbon Propulsion Systems (C-ALPS) EMC chamber (i.e., semi anechoic room, ISO 17025 approved and certified) from Coventry University, UK to reduce at minimum the potential external interferences, Fig. 2. To derive a comprehensive picture of the possible EM RF emissions encountered by a Hall sensor on a GaN transistor under load, seven transistor's gate switching frequencies of 1, 5, 10, 50, 100, 500 and 1000 kHz were selected for tests. Likewise, three different loads such as semiconductive, resistive, and inductive were selected to explore possible functioning variations generated by their distinct nature and voltage requirements. It was decided to use the ALS31001LUAATN three-pin linear analog output manufactured by Allegro Microsystems since its reliability and robustness were proven in previous research projects [40], [41], [42]. Furthermore, according to recent experiments using Transphorm's GaN transistors [43], [44], [45], TP65H150G4PS 650 V, 13 A and TP65H050WS 650 V, 36 A have been found to be most suitable for this study's testing. The semiconductive load consisting of an AMTECH S1583 24 LED flashlight requiring 5 V and 0.4 A, the inductive load based on a HP System Fan from a 532149-001 module, powered at 12 V and requiring 1.8 A and the resistive load composed of a 50 Ω resistor used at 24 V and dissipating approx. 0.06 A were chosen to study possible different behaviors of the GaN transistor induced at certain frequencies.

Although the initial study focused on evidencing the minimum B detectable via an external Hall sensor in close proximity to a functioning GaN transistor as an extension to

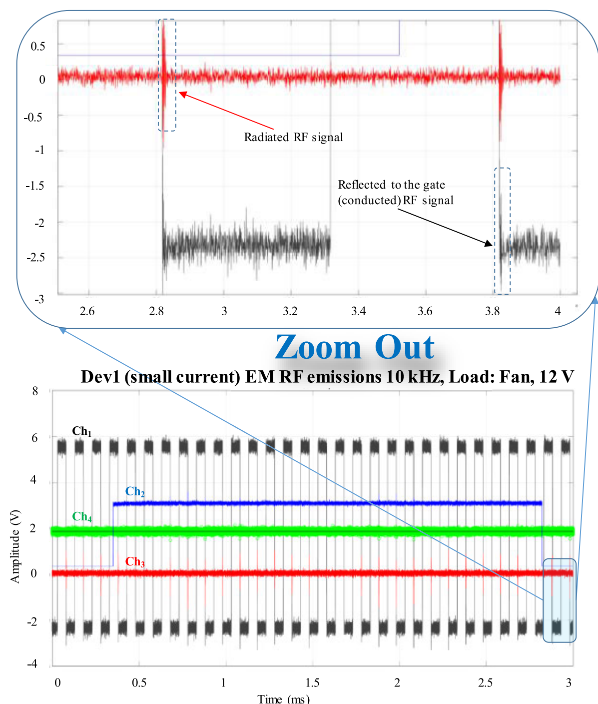

FIGURE 6. Oscilloscope monitoring on four channels (Ch): GaN transistor gate signal Ch_1 (black), microcontroller's data acquisition Ch_2 (blue), inductor coil RF noise Ch_3 (red), Hall sensor output Ch_4 (green).

[46] and [39], monitoring and recording the EM RF emissions at various frequencies and loads yielded a different set of independent findings. Consequently, the methodology section will be divided into two subsections: first, the interfacing and calibration setup for the Hall sensor will be discussed, and second, the EM RF emissions monitoring will be approached.

A. HALL SENSOR CALIBRATION AND PREPARATIONS

In conjunction with a set of permanent neodymium magnets, the magnetic field meter Extech SDL900 was used to provide the reference values for the Hall sensor interfaced by the microcontroller. Using a reversed plastic box, the round magnets were gradually pushed closer to the bottom-mounted magnetometer's probe. PIC24F16KA102 ADC module set to 500 kSa/s and 10 bits result conversion was used to interface the Hall sensor powered at 3.3 V, a general voltage used by low-power microcontrollers. The microcontroller's UART transceiver is linked to a PC serial communication port via a TTL−232R USB conversion cable produced by FTDI. MathWorks' MATLAB environment was used to receive, plot, and record the sensor data. Fig. 3 shows the schematic for the microcontroller's data acquisition board, derived from a wireless design presented in [47].

Since the data is delivered in the form of ADC voltage samples that take into account the sensor's position towards B, a transformation function is required. As it was established in [46], a linear conversion function can be derived from a polynomial line equation rather than from its parametric form which is better suited for vector analysis and modeling like encountered in ray tracing simulations [48]()() [49]. A first-order polyfit function can be used in MATLAB [50] since the function format is now known. Two measurement ranges have been used during calibration, Fig. 4, a short range thin grained between ±10 mT and a long range covering for the ±90 mT interval. It can be observed that the reversed box enclosing magnets produce linear results for the Hall sensor's middle detecting range (i.e., magneto-static far field). In contrast, as B varies with the cubic ratio of its distance from source, the extremities close to the saturation zones become unstable as it is difficult to match the imposed initial measurement step. Due to this, a calibration system with a nonlinear response will provide greater stability close to a strong magnet's field (i.e., a magneto-static near field) than one with a linear response, which must deliver consistent fine-grained steps.

The Hall sensor's output signal is also monitored by a RTM3004 5 GSa/s oscilloscope. The DC offset difference between the microcontroller and oscilloscope sensor's readings is approximatively 174 mV, Fig. 5. Due to higher sensitivity and sampling frequency, the oscilloscope exhibits a more significant measurement ripple in time domain of approx. 489 mV peak-to-peak (pp) as compared with the microcontroller's only 19 mV. Nevertheless, when transferring the measurements to frequency domain it can be clearly observed that both instrument's signals present the average DC component amplitude at 0 Hz whereas the energy stored in the high frequency ripple is three orders of magnitude lower. This demonstrates that both microcontroller and oscilloscope sensor's measurements can be achieved through these two methods: averaging in time domain or selecting the DC component at 0 Hz in frequency domain.

B. EM RF EMISSION MONITORING SETUP

The oscilloscope used for monitoring the Hall sensor readings also connects on its analog inputs the signal generator's commanding signal on the GaN transistor's gate, a signal generated by the microcontroller on pin RB7 after 10 ADC readings-converting-transmitting the data to the UART and an inductor placed 10 cm away from transistor, Fig. 6. The inductor is a planar coil IWAS4532AGEB140KF1 from Vishay and it is used as a recording probe for the EM RF emission while shared with a FPC1500 3 GHz bandwidth spectrum analyzer. The decision to employ the planar inductor (i.e., a small omnidirectional sensing element) as a probe to detect the switching RF emissions was made for two reasons: measure the near-field electromagnetic interferences that the Hall sensor and other proximity electronics may encounter, and minimize any antenna misalignments or demanding testing angles that a large broadband probe, such as a BiLog or BiConical antenna, may necessitate. The oscilloscope was used for recording the switching EM RF pulses amplitudes and timing whereas the spectrum analyzer was

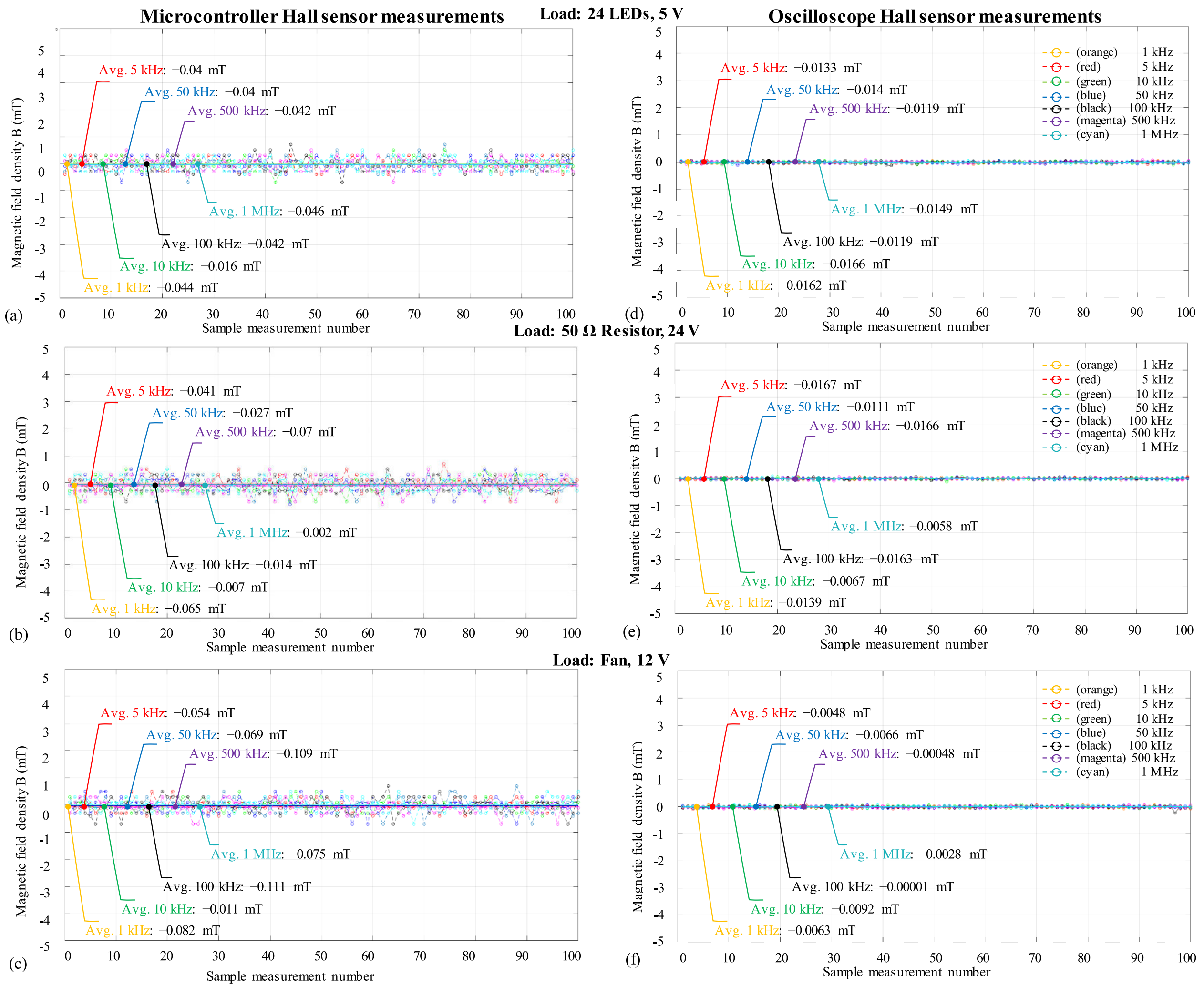

FIGURE 7. The Hall sensor's magnetic field measurements inside the EMC room during the GaN transistor functioning under three different loads, LEDs, resistor and fan, switching power at seven different frequencies of 1, 5, 10, 50, 100, 500, 1000 kHz: Hall sensor interfaced with the microcontroller (a) – (c) and the oscilloscope (d) – (f).

used for identifying the surrounding noise in the frequency domain.

The GaN transistor wasn't tested in its half-bridge configuration therefore, an additional 1N4007 diode was added in parallel with the load for a current path in the OFF state. As well, since the transistor's gate driver was replaced by the signal generator, a 1 MΩ pulldown resistor have been placed between transistor's gate and ground.

III. RESULTS AND DISCUSSION

The results and discussion section consists of three subsections. The first demonstrates the Hall sensor magnetic field measurement stability in close proximity to a functioning GaN transistor. By using an oscilloscope and a spectrum analyzer, the second section identifies the electrical parameter producing the switching noise and introduce a comparison case to outline how these phenomena are spatially interconnected. The last section delivers an explanation for the electrical switching radiated noise supported by the basic electrical power formula.

A. HALL SENSOR MAGNETIC FIELD SENSING

Fig. 7 illustrates the Hall sensor readings when interfaced with the microcontroller (a) – (c), and separately with the oscilloscope (d) – (f). Despite the fact that both instruments display average values very close to 0 mT, the microcontroller exhibits a higher variation when compared to the oscilloscope due to its lower acquisition speed and ADC conversions. Nevertheless, the resulted recorded values indicate that the sensor will not be influenced by the EM RF emissions resulted from the GaN transistor switching regime and if the sensor will be interfaced by a microcontroller then the minimum magnetic field sensed needs to be beyond ±1 mT threshold.

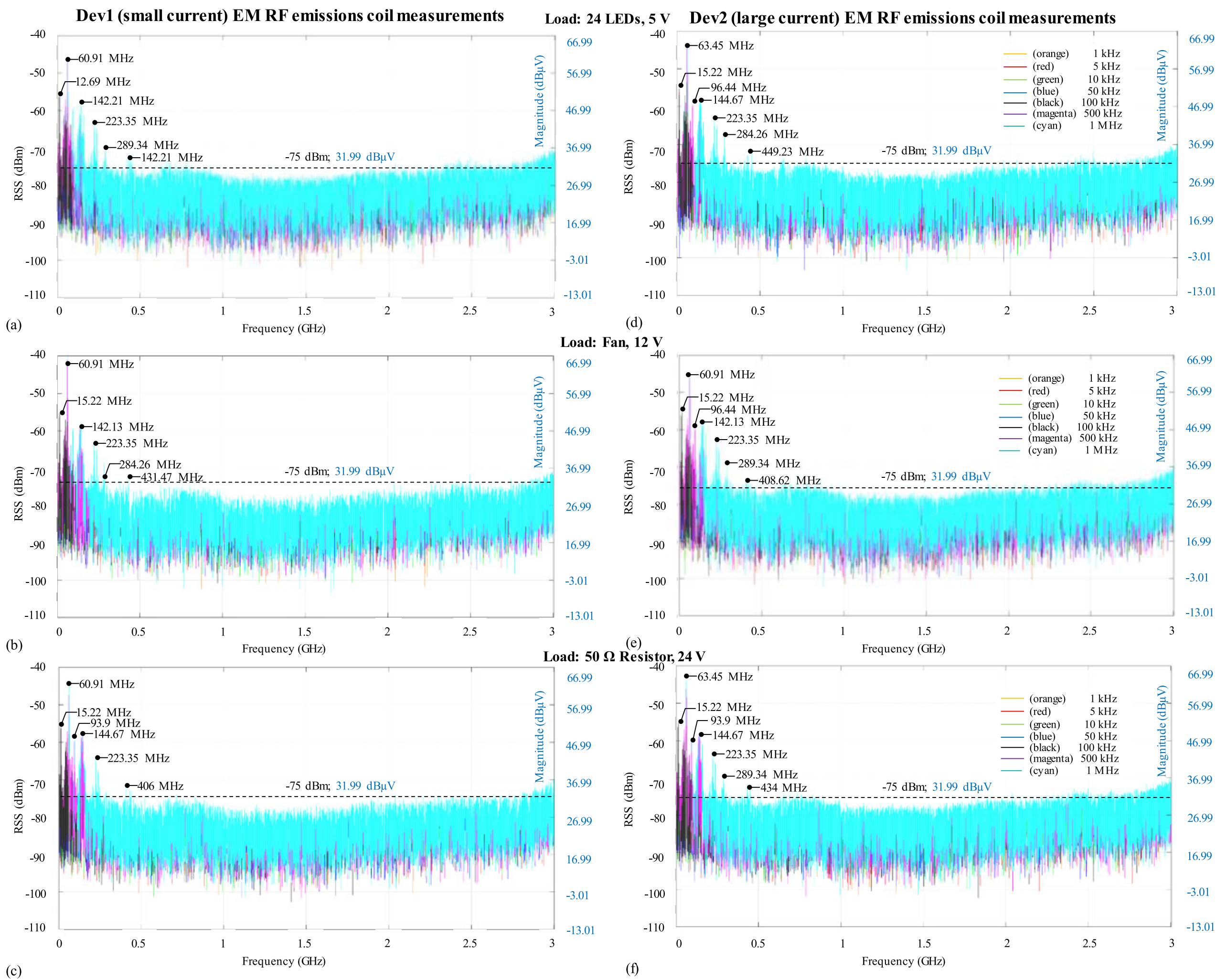

FIGURE 8. The EM RF noise recorded with the spectrum analyzer for two GaN transistors under load tested at seven: device one TP65H150G4PS 650 V 13 A (a) – (c), and device two TP65H050WS 650 V 36 A (d) – (f).

B. GaN TRANSISTOR SWITCHING NOISE MONITORING AND TIMMING

The EM RF emissions have been monitored by using both the spectrum analyzer and the oscilloscope. The spectrum analyzer results subtracted the initial noise before any of the instruments being ON therefore, the graphs from Fig. 8 are illustrating the received signal strength (RSS), where the signal is considered the EM RF emissions of the GaN transistor under various loads. Since the instrument has to cover a 3 GHz spectrum, the sharp emission bursts from the ON/OFF switching of GaN transistors cannot be captured due to its slow frequency sweeping. The spectrum analyzer measurements are strongly illustrating that most of the EM RF emissions higher than −75 dBm are localized in the lower side of the spectrum up to 500 MHz. It can be observed that the noise spikes caused by experimental setup instruments are typically centered around 15, 60, 90, 140, 220, 280 and 400 MHz. To deliver a clearer comparative view, the RSS expressed in dBm have been also expressed in dBμV (i.e., right vertical axis). Using the induction coil at 10 cm from the functioning GaN transistor, the spectrum analyzer shows a maximum amplitude of 6 mV noise spike at 60 MHz. According to Fig. 9, the oscilloscope connected to the same coil displays pulses that timed with GaN transistor switching at lower frequencies, thus completing the picture of EM RF emissions.

A similar GaN transistor, designed to handle approximately three times as much current as its previous counterpart, has been tested under similar conditions to better understand switching EM RF emissions. Whereas the general RSS was similar as for the first transistor, there was a significant difference in the switching noise recorded by the oscilloscope. When compared to its larger peers, the smaller current GaN transistor emits a considerable larger amount of electromagnetic RF emissions. As well, when analyzing the noise spike densities, it is evident that the highest amount is delivered by the load which consumes the highest current, the inductive fan, followed by the semiconductive LED and then

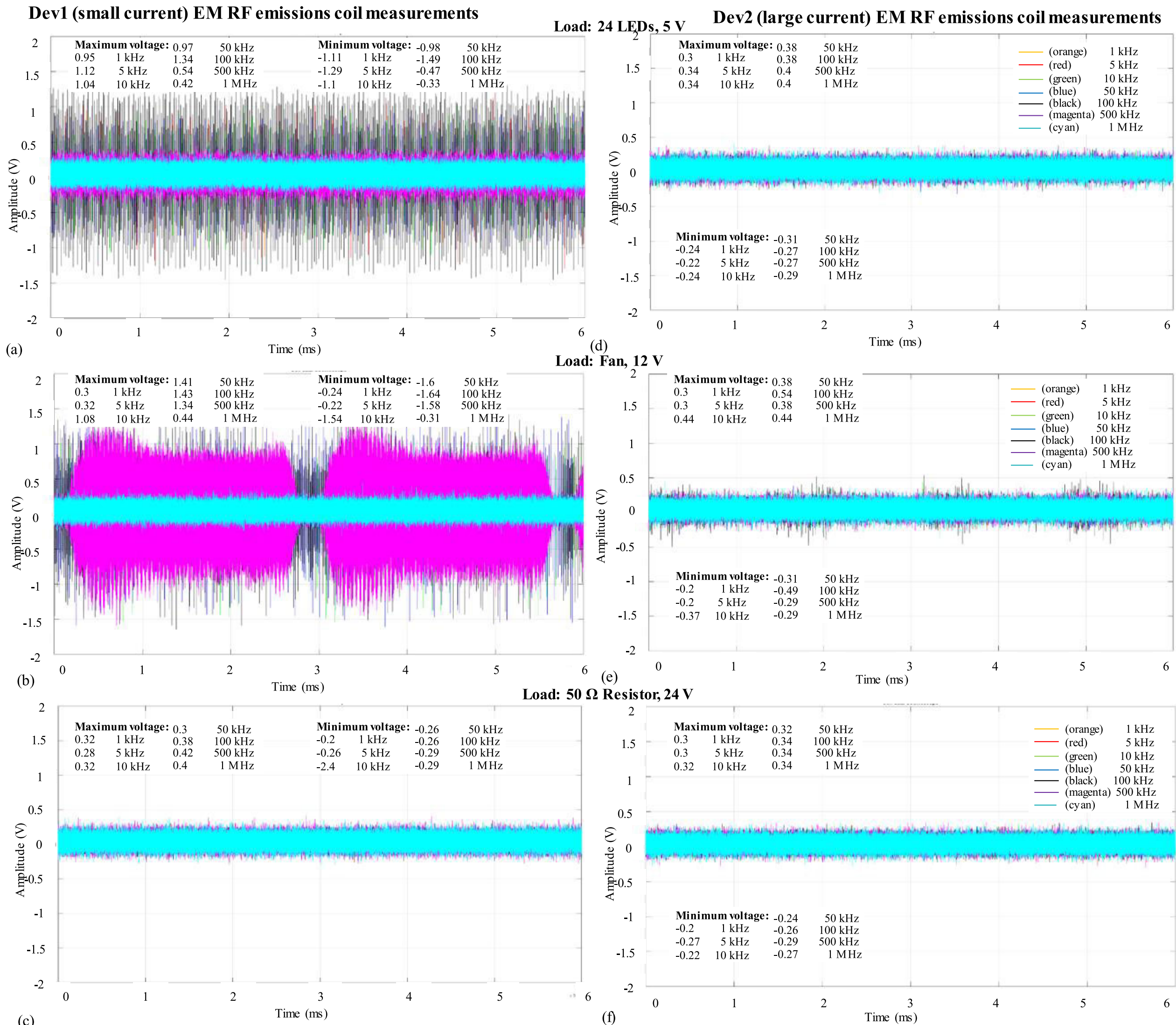

FIGURE 9. The EM RF noise recorded with the oscilloscope for two GaN transistors under load tested at seven: device one TP65H150G4PS 650 V 13 A (a) – (c), and device two TP65H050WS 650 V 36 A (d) – (f).

the resistor. According to both observations, EM RF switching emissions correlate directly with the switching current allowed by the GaN transistor and its quantity required by the various loads.

C. CAUSE FOR SWITCHING NOISE EM RF EMMISIONS

This section expands on the previous observations regarding the EM RF switching noise and explains it as a common phenomenon for all electrical switches. Hence, an illustrative figure depicting a classical mechanical moving lever electrical switch in parallel with a solid-state semiconductor transistor are showed in Fig. 10. By representing the current transfer as a high voltage electric arc such as in lighting or spark-gap devices, a more intuitive picture can be created to demonstrate the energy transfer between two electrified points: high voltage is a field capable of connecting two opposite voltage potential points by aligning and polarizing the charges between them. If the concentration of free electrons and ions between these two points is high enough, the dielectric/isolator will break, allowing current to flow, emitting light and heat along the path with the lowest resistance. In a similar manner to synchrotron radiations, the acceleration of charge carriers will produce a propagating electromagnetic wave. Low voltage fields will act on small distances between the two voltage potential differences however, allowing a variety of minimal resistance current paths to be found. Compared to the previous case, when the voltage is high, the dielectric breakdown between the two points acts on larger distances, resulting in very few or only one transfer points on the lowest current path. Often, the electric arc

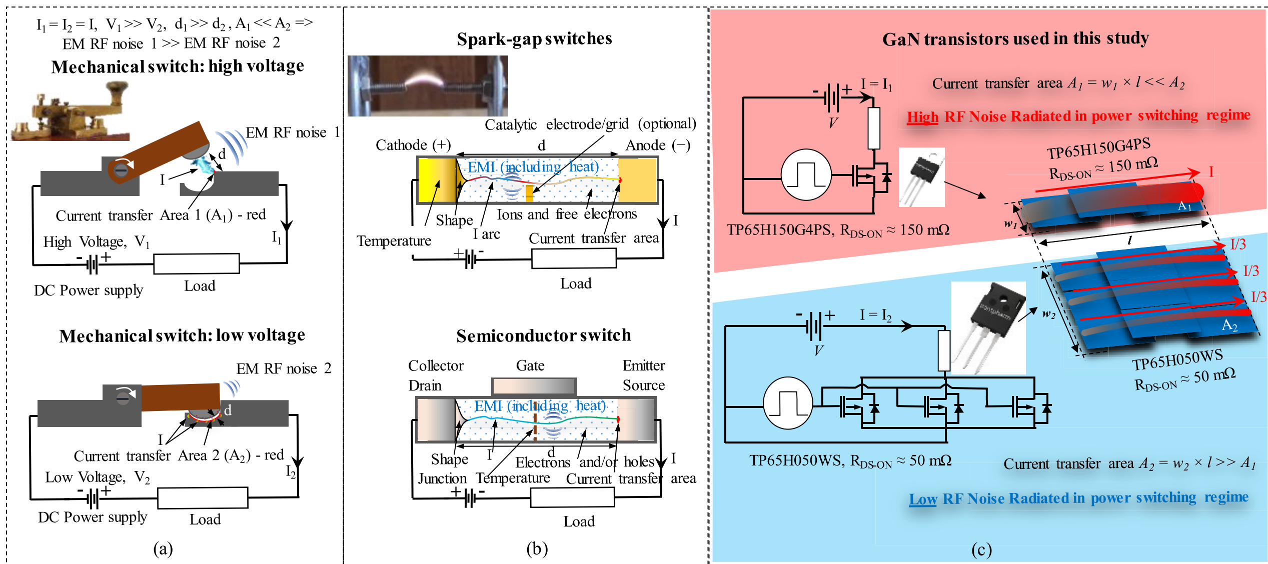

FIGURE 10. EM RF noise radiated by a mechanical switch at high and low voltage (a), electromagnetic interferences (EMI) radiated by a spark gap switch and a solid state semiconductor transistor (b). The two GaN transistors used in this study experimental work and their R_{DS-ON} area equivalent representation (c).

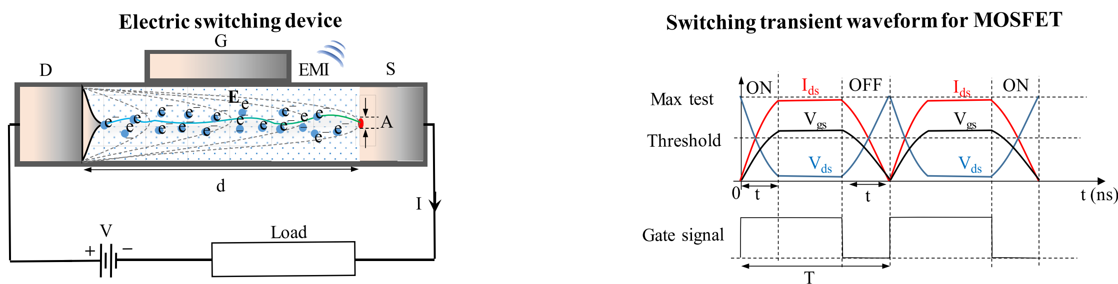

Electric switching power losses (total):

$$P_{switching} = \frac{1}{2} IV(t_{ON} + t_{OFF})f = IVtf = \frac{IVt}{T}$$

Electric switching EM radiated power losses based on Larmor formula, assuming that channel's electrons accelerate non-uniformly:

$$P_{switching\ radiated} = \frac{q^2a^2}{6\pi\varepsilon_0 c_0^3}(t_{ON} + t_{OFF})f = \frac{2eI^2Vt}{3\pi m_e \varepsilon_0 c_0^3 T} = \frac{2eI}{3\pi m_e \varepsilon_0 c_0^3} P_{switching} = 0.156 \cdot 10^{-3} \cdot I \cdot P_{switching}$$

FIGURE 11. Switching power loses for a transistor commanded on the gate with a square signal of frequency $f = 1/T$ while its idealized transient times $t_{ON} = t_{OFF} = t$. The total switching power loss, $P_{switching}$ is three order higher than delivered by Larmor formula for radiated power when the load current is under 10 A.

discharges accompanies long distances between the terminations of mechanical switches. However, in solid-state devices, the acceleration of the charges does not produce observable ionization plasma, so it is harder to observe the process "in action".

On the basis of the previous results and measurements, we infer that all electrical switches produce switching EM RF noise proportional to their conductive channel spatial dimensions without requiring special conditions. When comparing two similar devices, in this case switches, they will both operate at the same temperature and voltage but only their spatial physical conductive channel properties will determine EM RF emissions quantity.

The diversity of electric shapes, distances, materials, etc., makes it difficult to derive a formula delivering the amount of EM RF switching noise when parameters like current, voltage and temperature are similar for different electrical switches. Generally, it may be assumed that a larger current conduction channel will produce fewer radio emissions than a smaller one in the same conditions. It is possible to get an estimation of the total device's transient losses using

the traditional formula for electrical switching power losses [51], [52], however since that formula includes all possible dissipations, it could be two or three orders higher when considering only electromagnetic radiations. Therefore, the adjusted Larmor estimation formula [53], [54] may serve as a good starting point to calculate the EM radiations, as shown in Fig. 11. The formulae in the figure clearly demonstrate that if total transistor switching losses are on the order of Watts, the radiation derived from Larmor formulas is only on the order of mW for a current less than 10 A, and in the range of teens to hundreds of mW for a higher load current. The end result for radiated losses shows the dependence of the load current.

It is important to note two main observations in the context of power switching losses. Although this study design was to monitor the EM RF noises of a loaded GaN transistor while analyzing the behavior of a Hall sensor, the radiated emissions and the conclusions that the main generator is the switched load current perfectly align with previous EMC/EMI dedicated studies [55]. The second point as showed in this study for GaN transistors the emission is only on the switching OFF time, meaning that accelerated electrons on the Larmor formula will emit only when braking, this meaning that the constant coefficient in Fig. 11 breaks in half, making it even smaller.

IV. CONCLUSION

Since the vast majority of conducted and radiated EMI studies and reviews provide an extensive database of previous and current measures for reducing EM emissions, this study focused only on the noise levels and their possible mechanisms rather than their reduction; therefore, further research will be conducted on only this aspect.

The study's findings emphasise a few key aspects of a GaN power transistor's radiated EMI during the power switching:

- if the Hall sensor is integrated on a GaN power transistor chip for current monitoring, then it is recommended that a low power conductive loop supply a magnetic field density above ± 1 mT.
- through successive tests and instruments it was demonstrated that the GaN transistor EM RF emissions are due to the conducted current through its junction, and that a larger conducting area with a lower resistance will produce less radiated noise.
- it was delivered a straightforward explanation for all electrical switching radiated noise, which is caused by the conducted current's accelerated charges passing through a spatial area, whose size may reduce the noise if it is increased.
- the induced radiated EMI occurs when the transistor switches the power OFF, this aspect confirming the idea of potential emission from electron acceleration/deceleration process through Larmor principle.
- even at low power (i.e., maximum 24 V and less than 2 A), the radiated field can generate voltages up to 1.5 V in neighboring circuitry and devices, as proven by the receiving coil at 10 cm distance from the transistor.
- it was experimentally proven that the most significant radiated EMI spectrum and harmonics due to power switching up to 1 MHz occur between 0 and 500 MHz, and that their influence in the GHz region is negligible.

These fundamental insides may prove critical for anyone working with switching power transistors even at low and medium power levels. Furthermore, the experimental results given in this paper suggest that magnetic sensor designs should be evaluated if located near a power switch, in terms of potential noise floor versus measurement. Overall, in an environment like that required by e-mobility systems, where electric switching power supply drive motors whereas Hall magnetic sensors provide real-time feedback, this research can provide a significant step forward in performance, safety and design testing.

REFERENCES

[1] S. J. Hormozabad, M. G. Soto, and H. Adeli, "Integrating structural control, health monitoring, and energy harvesting for smart cities," *Expert Syst.*, vol. 38, no. 8, Dec. 2021, Art. no. e12845.

[2] Z. J. Chew, Y. Kuang, T. Ruan, and M. Zhu, "Energy harvesting in smart cities," in *Handbook of Smart Cities*. Cham, Switzerland: Springer, 2020, pp. 1–27.

[3] G. Shan, Y. Kuang, and M. Zhu, "Piezoelectric energy harvesting from rail track vibration using frequency up-conversion mechanism," *IFAC-PapersOnLine*, vol. 55, no. 27, pp. 218–223, 2022.

[4] V. Marsic, M. Zhu, and S. Williams, "Design and implementation of a wireless sensor communication system with low power consumption for energy harvesting technology," in *Proc. 19th Telecommun. Forum (TELFOR) Proc. Papers*, Nov. 2011, pp. 607–610.

[5] V. A. Marsic, *Wireless Sensor Communication System With Low Power Consumption for Energy Harvesting Technology*. Cranfield, U.K.: Cranfield Univ., 2012.

[6] V. Marsic, S. Faramehr, J. Fleming, P. Ball, S. Ou, and P. Igic, "Buried RF sensors for smart road infrastructure: Empirical communication range testing, propagation by line of sight, diffraction and reflection model and technology comparison for 868 MHz–2.4 GHz," *Sensors*, vol. 23, no. 3, p. 1669, Feb. 2023.

[7] C. Roman, R. Liao, P. Ball, S. Ou, and M. de Heaver, "Detecting on-street parking spaces in smart cities: Performance evaluation of fixed and mobile sensing systems," *IEEE Trans. Intell. Transp. Syst.*, vol. 19, no. 7, pp. 2234–2245, Jul. 2018, doi: 10.1109/TITS.2018.2804169.

[8] M. Bauer, L. Sanchez, and J. Song, "IoT-enabled smart cities: Evolution and outlook," *Sensors*, vol. 21, no. 13, p. 4511, Jun. 2021.

[9] J. Fleming, T. Amietszajew, J. Charmet, A. J. Roberts, D. Greenwood, and R. Bhagat, "The design and impact of in-situ and operando thermal sensing for smart energy storage," *J. Energy Storage*, vol. 22, pp. 36–43, Apr. 2019.

[10] T. Amietszajew, E. McTurk, J. Fleming, and R. Bhagat, "Understanding the limits of rapid charging using instrumented commercial 18650 high-energy Li-ion cells," *Electrochimica Acta*, vol. 263, pp. 346–352, Feb. 2018.

[11] J. Fleming, T. Amietszajew, and A. Roberts, "In-situ electronics and communications for intelligent energy storage," *HardwareX*, vol. 11, Apr. 2022, Art. no. e00294.

[12] E. Bassi, F. Benzi, L. Almeida, and T. Nolte, "Powerline communication in electric vehicles," in *Proc. IEEE Int. Electr. Mach. Drives Conf.*, May 2009, pp. 1749–1753.

[13] V. Marsic, T. Amietszajew, P. Igic, S. Faramehr, and J. Fleming, "Wireless communication test on 868 MHz and 2.4 GHz from inside the 18650 Li-ion enclosed metal shell," *Sensors*, vol. 22, no. 5, p. 1966, Mar. 2022.

[14] V. Marsic, T. Amietszajew, P. Igic, S. Faramehr, and J. Fleming, "DC power line communication (PLC) on 868 MHz and 2.4 GHz wired RF transceivers," *Sensors*, vol. 22, no. 5, p. 2043, Mar. 2022.

[15] V. Marsic, T. Amietszajew, C. Gardner, P. Igic, S. Faramehr, and J. Fleming, "Impact of Li-ion battery on system's overall impedance and received signal strength for power line communication (PLC)," *Sensors*, vol. 22, no. 7, p. 2634, Mar. 2022.

[16] M. J. Koshkouei, E. Kampert, A. D. Moore, and M. D. Higgins, "Impact of lithium-ion battery state of charge on in situ QAM-based power line communication," *Sensors*, vol. 22, no. 16, p. 6144, Aug. 2022.

[17] B. N. Pushpakaran, A. S. Subburaj, and S. B. Bayne, "Commercial GaN-based power electronic systems: A review," *J. Electron. Mater.*, vol. 49, no. 11, pp. 6247–6262, Nov. 2020.

[18] P. Igic, N. Jankovic, J. Evans, M. Elwin, S. Batcup, and S. Faramehr, "Dual-drain GaN magnetic sensor compatible with GaN RF power technology," *IEEE Electron Device Lett.*, vol. 39, no. 5, pp. 746–748, May 2018.

[19] S. Faramehr, P. Igic, and K. Kalna, "Modelling and optimization of GaN capped HEMTs," in *Proc. 10th Int. Conf. Adv. Semiconductor Devices Microsyst.*, Oct. 2014, pp. 1–4.

[20] S. Faramehr, K. Kalna, and P. Igic, "Modeling of 2DEG and 2DHG in i-GaN capped AlGaN/AlN/GaN HEMTs," in *Proc. 29th Int. Conf. Microelectron. (MIEL)*, May 2014, pp. 81–84.

[21] A. Videt, K. Li, N. Idir, P. Evans, and M. Johnson, "Analysis of GaN converter circuit stability influenced by current collapse effect," in *Proc. IEEE Appl. Power Electron. Conf. Expo. (APEC)*, Mar. 2020, pp. 2570–2576.

[22] P. B. Derkacz, J.-L. Schanen, P.-O. Jeannin, P. J. Chrzan, P. Musznicki, and M. Petit, "EMI mitigation of GaN power inverter leg by local shielding techniques," *IEEE Trans. Power Electron.*, vol. 37, no. 10, pp. 11996–12004, May 2022.

[23] B. Zhang and S. Wang, "An overview of wide bandgap power semiconductor device packaging techniques for EMI reduction," in *Proc. IEEE Symp. Electromagn. Compat., Signal Integrity Power Integrity (EMC, SI PI)*, Jul. 2018, pp. 297–301.

[24] W. J. Zhang, Y. Leng, J. Yu, Y. S. Lu, C. Y. Cheng, and W. T. Ng, "An integrated gate driver for E-mode GaN HEMTs with active clamping for reverse conduction detection," in *Proc. 31st Int. Symp. Power Semiconductor Devices ICs (ISPSD)*, May 2019, pp. 83–86.

[25] P. K. Prasobhu, V. Raveendran, G. Buticchi, and M. Liserre, "Active thermal control of GaN-based DC/DC converter," *IEEE Trans. Ind. Appl.*, vol. 54, no. 4, pp. 3529–3540, Jul. 2018.

[26] S. Faramehr, N. Janković, and P. Igić, "Analysis of GaN MagHEMTs," *Semicond. Sci. Technol.*, vol. 33, no. 9, Sep. 2018, Art. no. 095015.

[27] S. Faramehr, B. R. Thomas, N. Jankovic, J. E. Evans, M. P. Elwin, and P. Igic, "Analysis of GaN MagFETs compatible with RF power technology," in *Proc. 41st Int. Conv. Inf. Commun. Technol., Electron. Microelectron. (MIPRO)*, May 2018, pp. 50–53.

[28] A. Hassan, Y. Savaria, and M. Sawan, "GaN integration technology, an ideal candidate for high-temperature applications: A review," *IEEE Access*, vol. 6, pp. 78790–78802, 2018.

[29] S. Bentley, X. Li, D. A. J. Moran, and I. G. Thayne, "Fabrication of 22nm T-gates for HEMT applications," *Microelectron. Eng.*, vol. 85, nos. 5–6, pp. 1375–1378, May 2008.

[30] S. Zaima, "Technology evolution for silicon nanoelectronics: Postscaling technology," *Jpn. J. Appl. Phys.*, vol. 52, no. 3R, Mar. 2013, Art. no. 030001.

[31] C. Dang, A. Lu, H. Wang, H. Zhang, and Y. Lu, "Diamond semiconductor and elastic strain engineering," *J. Semiconductors*, vol. 43, no. 2, Feb. 2022, Art. no. 021801.

[32] K. G. Crawford, I. Maini, D. A. Macdonald, and D. A. J. Moran, "Surface transfer doping of diamond: A review," *Prog. Surf. Sci.*, vol. 96, no. 1, Feb. 2021, Art. no. 100613.

[33] O. Trescases, S. K. Murray, W. L. Jiang, and M. S. Zaman, "GaN power ICs: Reviewing strengths, gaps, and future directions," in *IEDM Tech. Dig.*, Dec. 2020, pp. 27.4.1–27.4.4.

[34] H. Majima, H. Ishihara, K. Ikeuchi, T. Ogawa, Y. Sawahara, T. Ogawa, S. Takaya, K. Onizuka, and O. Watanabe, "Cascoded GaN half-bridge with 17 MHz wide-band galvanically isolated current sensor," *Jpn. J. Appl. Phys.*, vol. 61, no. SC, May 2022, Art. no. SC1052.

[35] M. Biglarbegian, N. Kim, T. Zhao, and B. Parkhideh, "Development of isolated SenseGaN current monitoring for boundary conduction mode control of power converters," in *Proc. IEEE Appl. Power Electron. Conf. Expo. (APEC)*, Mar. 2018, pp. 2725–2729.

[36] P. Igic, O. Kryvchenkova, S. Faramehr, S. Batcup, and N. Jankovic, "High sensitivity magnetic sensors compatible with bulk silicon and SOI IC technology," in *Proc. IEEE 30th Int. Conf. Microelectron. (MIEL)*, Oct. 2017, pp. 55–59.

[37] S. Faramehr, N. Poluri, P. Igic, N. Jankovic, and M. M. De Souza, "Development of GaN transducer and on-chip concentrator for galvanic current sensing," *IEEE Trans. Electron Devices*, vol. 66, no. 10, pp. 4367–4372, Oct. 2019.

[38] B. R. Thomas, S. Faramehr, D. C. Moody, J. E. Evans, M. P. Elwin, and P. Igic, "Study of GaN dual-drain magnetic sensor performance at elevated temperatures," *IEEE Trans. Electron Devices*, vol. 66, no. 4, pp. 1937–1941, Apr. 2019.

[39] V. Marsic, S. Faramehr, and P. Igic, "Coil design for integration with GaN Hall-effect sensors," in *Proc. IEEE Workshop Wide Bandgap Power Devices Appl. Eur. (WiPDA Eur.)*, Sep. 2022, pp. 1–5.

[40] S. Jung, B. Lee, and K. Nam, "PMSM control based on edge field measurements by Hall sensors," in *Proc. 25th Annu. IEEE Appl. Power Electron. Conf. Expo. (APEC)*, Feb. 2010, pp. 2002–2006.

[41] Z. Wang, L. Banszerus, M. Otto, K. Watanabe, T. Taniguchi, C. Stampfer, and D. Neumaier, "Encapsulated graphene-based Hall sensors on foil with increased sensitivity," *Phys. Status Solidi B*, vol. 253, no. 12, pp. 2316–2320, Dec. 2016.

[42] B. A. Tuan, A. de Souza-Daw, H. M. Phuong, T. M. Hoang, and N. T. Dzung, "Magnetic camera for visualizing magnetic fields of home appliances," in *Proc. IEEE 5th Int. Conf. Commun. Electron. (ICCE)*, Jul. 2014, pp. 370–375.

[43] Z.-H. Huang, S.-W. Tang, C.-T. Fan, M.-C. Lin, and T.-L. Wu, "Dynamic on-resistance stability of SiC and GaN power devices during high-frequency (100–300 kHz) hard switching and zero voltage switching operations," *Microelectron. Rel.*, vol. 145, Jun. 2023, Art. no. 114983.

[44] E. O. Prado, P. C. Bolsi, H. C. Sartori, and J. R. Pinheiro, "An overview about Si, superjunction, siC and GaN power MOSFET technologies in power electronics applications," *Energies*, vol. 15, no. 14, p. 5244, Jul. 2022.

[45] Y. Zhang, J. Li, J. Wang, T. Q. Zheng, and P. Jia, "Dynamic-state analysis of inverter based on cascode GaN HEMTs for PV application," *Energies*, vol. 15, no. 20, p. 7791, Oct. 2022.

[46] V. Marsic, S. Faramehr, J. Fleming, R. Bhagat, and P. Igic, "Understanding the limits of a Hall sensor sensitivity for integration on a GaN power transistor chip: Experiments with market available components," in *Proc. 12th Int. Conf. Power Electron., Mach. Drives (PEMD)*, 2023, pp. 350–356.

[47] V. Marsic, E. Kampert, and M. D. Higgins, "Position discrimination of a 2.4 GHz IEEE 802.15.4 RF mobile source inside-outside a vehicle," in *Proc. Int. Conf. Smart Appl., Commun. Netw. (SmartNets)*, Sep. 2021, pp. 1–6.

[48] V. Marsic, E. Kampert, and M. D. Higgins, "Ray tracing 3D source modelling for optical reflectance sensing with wireless ranging application," in *Proc. IEEE Int. Symp. Robotic Sensors Environ. (ROSE)*, Oct. 2021, pp. 1–8.

[49] V. Marsic. (2022). *Detecting From In-vehicle At the Physical Layer a Smart Device Spatial Location Via 2.4 GHz SRD RF Services Innovation Report*. Univ. Warwick. [Online]. Available: http://wrap.warwick.ac.uk/167525

[50] A. Stahel, *Octave and MATLAB for Engineering Applications*. Cham, Switzerland: Springer, 2022.

[51] Y. Xiong, S. Sun, H. Jia, P. Shea, and Z. John Shen, "New physical insights on power MOSFET switching losses," *IEEE Trans. Power Electron.*, vol. 24, no. 2, pp. 525–531, Feb. 2009.

[52] M. A. Azpúrua, M. Pous, and F. Silva, "Time- and frequency-domain characterization of switching losses in GaN FETs power converters," *IEEE Trans. Power Electron.*, vol. 37, no. 3, pp. 3219–3232, Mar. 2022.

[53] A. Y. Shiekh and C. C. Vuille, "Does a charge in a uniform gravity field radiate? (The accelerating charge Paradox)," *Eur. Phys. J. Plus*, vol. 137, no. 10, p. 1179, Oct. 2022.

[54] S. Humphries, *Principles of Charged Particle Acceleration*. Chelmsford, MA, USA: Courier Corporation, 2013.

[55] Y. Zhang, S. Wang, and Y. Chu, "Analysis and comparison of the radiated electromagnetic interference generated by power converters with Si MOSFETs and GaN HEMTs," *IEEE Trans. Power Electron.*, vol. 35, no. 8, pp. 8050–8062, Aug. 2020.

VLAD MARSIC received the B.Eng. degree in communication from the Faculty of Electronics and Telecommunications, Gheorghe Asachi Technical University, Romania, in 2002, the M.Sc. degree in low power RF sensing from the School of Applied Sciences (SAS), Cranfield University, U.K., in 2012, and the Eng.D. degree in RF communication and location services from the Warwick Manufacturing Group (WMG), University of Warwick, U.K., in 2019. From 2003 to 2011, he was performed various roles in industry, such as an Automotive Electronic Diagnosis Engineer and a 3G RAN Engineer of IT support, from 2012 to 2022, he joined the Academia Environment as a KTP RF Engineer with Oxford Brookes University, U.K., a System Engineer with WMG, U.K., and a Research Fellow with Cranfield University and Coventry University, U.K. His research interests include the experimental RF areas of remote sensing, wireless networks, radio location, power line communication (PLC) and theoretical electromagnetic simulation, analysis techniques supported and developed through MATLAB, C/C++, Spice, and NI LabVIEW. He was nominated and received the Best Paper Award in various conferences and symposiums, where he presented and authored original research work in the RF experimental and modelling domains.

SOROUSH FARAMEHR received the M.Sc. and Ph.D. degrees in electrical engineering from Swansea University, Swansea, U.K., in 2011 and 2015, respectively. In 2019, he joined Coventry University, Coventry, U.K. He is currently an Associate Professor with the Centre for Advanced Low-Carbon Propulsion Systems, Coventry University, and the Team Lead of Integrated Electrical and Electronic Systems. His research interest includes more efficient electronic devices to leave less carbon footprint on the environment.

JOE FLEMING received the M.Sc. degree in electronic engineering from De Montfort University, Leicester, U.K., in 2012, and the Ph.D. degree in engineering from the University of Warwick, Coventry, U.K., in 2018.

He is currently an Assistant Professor with Coventry University and was a former Lead Engineer with the University of Warwick and Alert-iT Care Alarms. He has over ten years of theory, design and experimental development experience of bespoke electronic systems, sensors, and instrumentation, for both academic and industrial applications. His principle research interests include sensors, communications, and system integration. Since 2015, he has been developing a broad portfolio of research aimed at improving the performance and understanding of the limits of energy storage, through the use of embedded electronics and sensors. Consequently, the main achievement, since he joined academia is to have established an international reputation for instrumented energy storage and to have produced fundamental high impact research, which has a direct and current benefit to the energy storage sector.

ROHIT BHAGAT is currently the Chair of Electrochemical Energy Storage and the Centre Director of the E-Mobility Research Centre, Coventry University (CU). He specializes in the characterization and optimization of processes, systems, and devices through application of electrochemical techniques and materials knowledge. He is a PI/Co-I of several energy storage research projects worth >£37m including EPSRC Grants (EP/N509863/1, EP/N001583/1, and EP/M009394/1) and Innovate U.K. Grants (TS/N009428/1, TS/N004558/1, and TS/N00373X/1). He has led several research projects focused on lithium battery manufacturing and characterization methods. He has 60 publications with an H-index of 25.

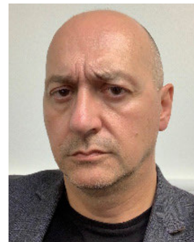

PETAR IGIC received the Dipl.-Eng. and Mag.Sc. degrees in electrical and electronics engineering from the University of Nis, Nis, Serbia, in 1993 and 1997, respectively, and the Ph.D. degree from Swansea University, Swansea, Wales, U.K., in 2000.

From 2000 to 2018, he was with the College of Engineering, Swansea University, where he was an Academic Member of Staff, the EEE Director of Study, and the Director of the College's Electronic Systems Design Centre. He is currently a Full Professor with the Centre for Advanced Low Carbon Propulsion Systems (C- ALPS), CGFM, Coventry University, England, U.K. His main research interests include Si and WBG power semiconductor applications for energy conversion in automotive industry and renewable energy applications.